DOI 10.1007/s10812-016-0273-6
Journal of Applied Spectroscopy, Vol. 83, No. 2, May, 2016 (Russian Original Vol. 83, No. 2, March–April, 2016)

INFLUENCE OF MAGNETIC LOSSES ON MICROWAVE ABSORPTION BY CARBON-NANOTUBE NANOCOMPOSITES WITH A LOW CONCENTRATION OF FERROMAGNETIC NANOPARTICLES

A. V. Avramchuk,[a] M. M. Kasperovich,[a] N. A. Pevneva,[a]
A. V. Gusinsky,[a] O. V. Korolik,[b] M. S. Tivanov,[b]
B. G. Shulitski,[a] V. A. Labunov,[a] A. L. Danilyuk,[a]
I. V. Komissarov,[a] and S. L. Prischepa[a*]

UDC 620.3

The absorption properties of magnetic nanocomposites based on carbon nanotubes with a low concentration of ferromagnetic nanoparticles have been investigated in the 78–118 GHz frequency range. A correlation was established between the absorption properties of the nanocomposites and the character of the magnetostatic interaction between nanoparticles.

Keywords: *nanocomposite, microwave, carbon nanotubes, ferromagnetic nanoparticles, chemical vapor deposition.*

Introduction. Magnetic nanocomposites consisting of ferromagnetic nanoparticles (NP) incorporated into a matrix are currently being extensively investigated. A feature of such materials is the ability to control their properties using external stimuli, e.g., a magnetic field, spin-polarized current, or electromagnetic field. Magnetic properties in ordinary magnetic materials are determined by the domain structure and the domain boundaries within a grain. The magnetic properties and the static and dynamic magnetic behavior in nanostructured materials are determined by several factors responsible for the dominance of dipole, exchange, or anisotropic interaction between NP. Understanding and control of these interactions make it possible to design a new class of devices with improved operational characteristics and functional capabilities. Such magnetic nanocomposites are promising for information storage devices and emitting and high-frequency instruments.

New magnetic nanocomposites based on carbon nanotubes (CNT) are very promising for high-frequency applications such as transmission lines, detectors, antennas, and absorbing materials. The absorbing properties of CNT nanocomposites are determined mainly by ohmic and dielectric losses. However, intercalated magnetic NP in a CNT matrix increase the absorption of nanocomposites because of magnetic losses. Experimental investigations are needed and theoretical approaches that consider various parameters of the nanocomposites must be developed for a deeper understanding of the interaction mechanisms of electromagnetic radiation and CNT nanocomposites.

The goal of the present work was to establish the influence of changing the magnetic interaction between ferromagnetic NP intercalated into a CNT matrix on the microwave-absorbing properties of the nanocomposite. For this, the absorption of nanocomposites with a low concentration of ferromagnetic NP localized in the CNT matrix were studied by measuring the frequency dependences of the reflection and transmission coefficients in the range 78–118 GHz. The concentration of ferromagnetic NP was set by the concentration C_F of ferrocene [$Fe(C_5H_5)_2$] in a ferrocene–*o*-xylene mixture during chemical vapor deposition (CVD) of the CNT. It was recently found [1, 2] that the NP magnetic anisotropy is substantial for $C_F < 1\%$ and dominates over exchange coupling. The principal NP interaction mechanism for $C_F \geq 1\%$ is exchange coupling.

Experimental. CNT bundles were grown at 875°C in a stream of Ar (280 cm^3/min) for 1 min using a solution of ferrocene in *o*-xylene with $C_F = 0.6–1.0\%$. Thus, only one (C_F) of the many CVD processing parameters was varied. It was found earlier [2, 3] that the ferrocene concentration affected not only the concentration of ferromagnetic NP but also their average diameter, localization, and stoichiometric composition. Silicon plates [KDB 12 (111), 2.4 × 1.2 mm) were used as the substrates. The substrate dimensions were determined by the microwave-waveguide geometry.

*To whom correspondence should be addressed.

[a]Belarusian State University of Informatics and Radioelectronics, 6 P. Brovka Str., Minsk, 220013, Belarus; e-mail: prischepa@bsuir.by; [b]Belarusian State University, Minsk, Belarus. Translated from Zhurnal Prikladnoi Spektroskopii, Vol. 83, No. 2, pp. 244–248, March–April, 2016. Original article submitted October 5, 2015.

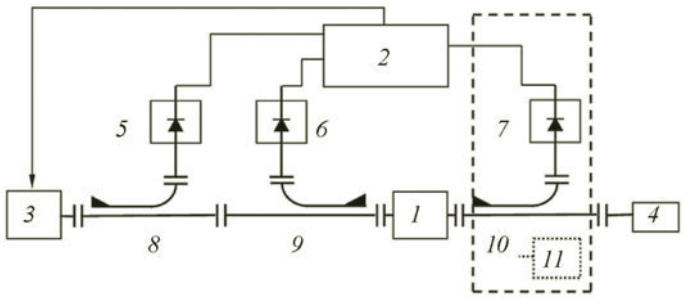

Fig. 1. Connection diagram for measurement system: sample to be measured (1), indicator (2), oscillating frequency generator (3), matched load (4), detectors and directional branchers for incident, reflected, and transmitted waves, respectively (5–7 and 8–10), short circuit used to calibrate the reflection coefficient (11); unit 11 must be turned off in reflection-coefficient measurement mode.

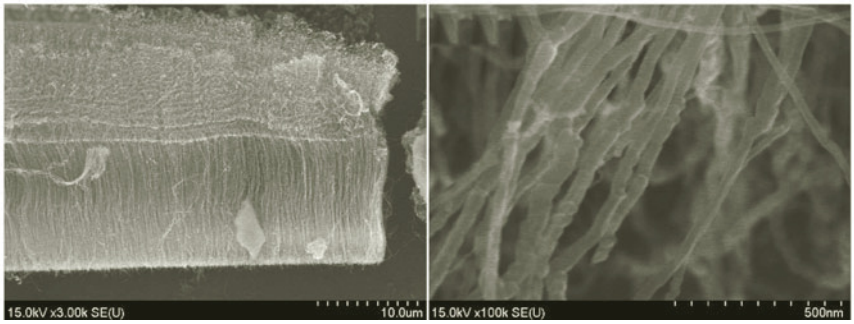

Fig. 2. Transverse cross sections of CNT prepared with ferrocene concentration C_F = 0.6% at different magnifications.

The structures of the CNT bundles were studied on a Hitachi S4800 scanning electron microscope (Japan). Raman scattering (RS) was investigated on a NanoFinder®HE scanning confocal microscope with spectral resolution 3 cm^{-1} in reverse scattering geometry and normal conditions. A laser with excitation energy 2.62 eV (473 nm) was used.

Frequency dependences of the coefficients of reflection and direct transmission (attenuation of electromagnetic radiation) of the CNT bundles were studied in the range 78–118 GHz using a panoramic attenuation meter and a KSVN RR2-01 (waveguide inner cross section 2.4 × 1.2 mm) consisting of a GKCh-61 generator, Ya2R-70 indicator, and measurement system. Figure 1 shows a diagram of the reflection and transmission coefficient measurement system.

Measurements were made using a waveguide method. For this, the sample was placed into a section of rectangular waveguide, the inner cross section of which was filled completely perpendicular to the propagation direction of the electromagnetic wave. Then, the waveguide section with the sample placed in it was inserted into the measurement system (Fig. 1). A closed system for passing the electromagnetic wave through the sample was designed in this manner. Special requirements were applied to the surface smoothness, sample size, and angle accuracy during sample preparation. Preference was given to a tight fit.

Results and Discussion. Figure 2 shows an example of the cross-sectional structure of a CNT sample synthesized with ferrocene concentration C_F = 0.6%. The obtained CNT bundles with a height of 20–30 μm were oriented primarily vertically. According to transmission electron microscopy, the ferromagnetic NP in samples with C_F < 0.8% were located in CNT cavities and were crystalline and coated with carbon. Their phase composition corresponded to iron (α-Fe) or cementite (Fe_3C) [1]. The characteristic size was determined by the CNT diameter and was Ø ≈ 20–30 nm [1, 3, 4]. NP were localized both between layers in walls and outside CNT for samples synthesized with C_F > 0.8% [3]. The nanocomposite was demonstrated to be ferromagnetic by measuring the specific magnetization, Curie temperature, and hysteresis loop over a broad temperature range of 4–350 K [1, 2]. The ferromagnetic NP were single-domain because, according to the literature [5], the diameter of a single-domain particle $2R_0$ is determined by exchange-coupling constant A and saturation magnetization M_{sat} as $2R_0 = 1.9 \cdot 30A/\mu_0 M_{sat}^2$. For our samples, this gives $2R_0 \approx 20$ nm using the published parameters [1]. The resulting single-domain value agreed well with the average diameter of 20–30 nm for NP intercalated into the CNT matrix synthesized with $C_F \leq 1\%$ [4].

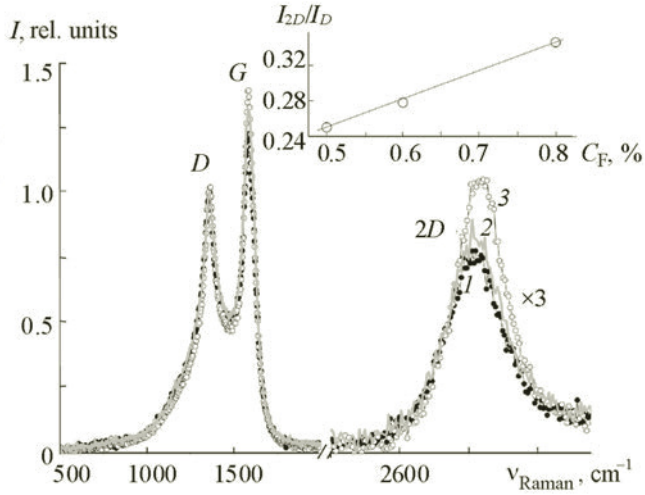

Fig. 3. Normalized Raman spectra of samples synthesized with C_F = 0.5 (1), 0.6 (2), and 0.8% (3).

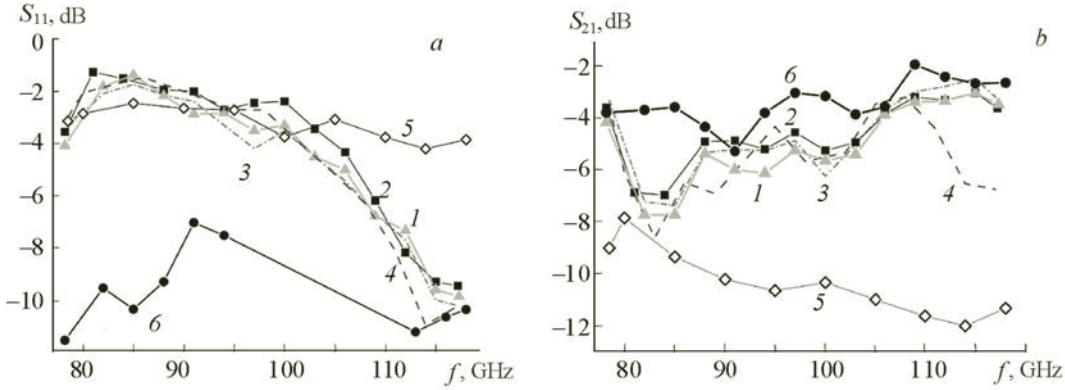

Fig. 4. Frequency dependences of coefficients of reflection S_{11} (a) and transmission S_{21} (b) of nanocomposites based on CNT synthesized with ferrocene concentrations 0.5 (1), 0.6 (2), 0.7 (3), 0.8 (4), and 1.0% (5) and blank substrate (6).

Figure 3 shows Raman spectra in the range 1000–3000 cm^{-1} for samples synthesized with C_F = 0.5–0.8%. Three main bands were observed, i.e., *D* (~1357 cm^{-1}) corresponding to disruptions of the graphite layer hexagonal structure; graphite-like band *G* (~1580 cm^{-1}); and band 2*D* (2715 cm^{-1}) that corresponded to double the frequency of defect band *D*. The Raman spectrum of each sample was normalized to the amplitude of peak *D*. According to the literature [6], the degree of CNT structure defectiveness could be estimated from the intensity ratio I_{2D}/I_D with higher ratios corresponding to a more perfect structure. The inset in Fig. 3 shows that the intensity ratio increased linearly with C_F. This is usually associated with improved quality of the graphite structure. Reduced CNT defectiveness was associated with increased DC conductivity [7].

Figure 4 shows frequency dependences of the coefficients of reflection (S_{11}) and transmission (S_{21}) of electromagnetic radiation by the CNT nanocomposites synthesized with different C_F. The contribution of the substrate on which the CNT bundles were grown had to be estimated before the coefficients of reflection and transmission of the CNT bundles with ferromagnetic NP could be measured. For this, parameters S_{11} and S_{21} of blank KDB 12 (111) silicon substrate were measured first. In this instance, ohmic and dielectric losses (specific DC conductivity of the substrate $\sigma = 0.083\ \Omega^{-1}\cdot cm^{-1}$) were largely responsible for the interaction mechanism of the incident electromagnetic wave with the substrate. The dielectric permittivity ε is related to specific conductivity σ by the standard equation:

$$\varepsilon(\omega) = \varepsilon'(\omega) - i\sigma/\omega\ ,$$

where ω is the cycle frequency; *i*, the imaginary unit. The real part of the dielectric permittivity (ε′) determines the material polarizability (dielectric losses); the term σ/ω, the ohmic losses.

The specific conductivity measured by the Van-der-Paauw method of CNT bundles synthesized with low ferrocene concentrations (C_F < 1%) was ~10 $\Omega^{-1}\cdot cm^{-1}$ [7]. This was more than two orders of magnitude greater than that of the substrates. The electromagnetic wave should have been reflected more by the CNT bundles than by the substrate. In fact, Fig. 4a shows that the reflection coefficients of the samples fell in the range from –4 to –2 dB for 80–100 GHz. The substrate reflection coefficient was –10 dB. However, the reflection coefficients of four samples synthesized with C_F = 0.5, 0.6, 0.7, and 0.8% decreased at frequencies >100 GHz to values typical of the substrate (–10 dB). The reflection coefficient did not drop for the sample with a higher concentration of ferromagnetic NP (C_F = 1.0%), a different type of localization (not only within the CNT but also outside them), and exchange coupling predominating over magnetic anisotropy and remained at about –4 dB even at a frequency >100 GHz. The electromagnetic radiation transmission coefficient through CNT bundles synthesized with ferrocene concentrations C_F = 0.5, 0.6, 0.7, and 0.8% were from –8 to –4 dB and tended to increase smoothly with frequency. However, Fig. 4 shows that the transmission coefficient for CNT bundles was always less than that of the blank silicon substrate. This could indicate that the CNT bundles were efficient absorbers of the electromagnetic wave.

An unusual sharp drop of the reflection coefficient was observed at frequencies >100 GHz for samples with low concentrations of ferromagnetic NP localized mainly within CNT. The dramatic change of reflectivity could be due to resonance effects caused by the complicated composite internal structure. In particular, it was shown [8] that a CNT nanocomposite with ferromagnetic NP could be described in terms of resistor–inductor–capacitor (*RLC*) resonance contours at frequencies >100 GHz. The resonant frequencies of these contours fall in the microwave region for reasonable capacitances and inductances (picofarads and picohenrys). This changes the polarizability of the magnetic dipole interacting with the *RLC*-contour impedance. As a result, the magnetic permeability of the whole nanocomposite depends quite erratically on frequency. Thus, the frequency dependence of the nanocomposite reflection coefficient is complicated with valleys and peaks [8].

Both the values and frequency dependence of the transmission coefficient for the sample with the higher concentration of ferromagnetic NP, a different localization pattern, and predominance of exchange coupling (C_F = 1%) differed in principle from those for samples with a lower concentration of ferromagnetic NP, localization only within CNT, and a substantial contribution of magnetic anisotropy. Figure 4 shows that the transmission coefficient for the sample with C_F = 1% decreased from –8 dB at 80 GHz to –12 dB at 115 GHz. Considering that the reflection coefficient for this sample was practically independent of frequency, the reduced transmission coefficient means that the absorption increased. This effect was naturally associated with increased magnetic losses at magnetic dipoles formed by ferromagnetic NP distributed in the CNT matrix.

Conclusions. The absorbance properties of CNT magnetic nanocomposites in the frequency range 78–118 GHz were found to be correlated with the magnetostatic interaction between the ferromagnetic NP. The reflection coefficient dropped sharply whereas the transmission coefficient increased smoothly at frequencies >100 GHz if magnetic anisotropy dominated. The absorption of electromagnetic radiation increased. The reflection coefficient was practically constant in the studied frequency range in the sample with predominantly exchange coupling between ferromagnetic NP. However, the transmission coefficient decreased smoothly due to increased absorption at increased frequency. Despite the increased absorption, the mechanism for all samples depended on the type of magnetic interaction between the NP.

REFERENCES

1. A. L. Danilyuk, A. L. Prudnikava, I. V. Komissarov, K. I. Yanushkevich, A. Derory, F. Le Normand, V. A. Labunov, and S. L. Prischepa, *Carbon*, **68**, 337–345 (2014).
2. S. L. Prischepa, A. L. Danilyuk, A. L. Prudnikava, I. V. Komissarov, V. A. Labunov, and F. Le Normand, *Phys. Status Solidi C*, **11**, Nos. 5–6, 1074–1079 (2014).
3. S. L. Prischepa, A. L. Danilyuk, A. L. Prudnikava, I. V. Komissarov, V. A. Labunov, K. I. Yanushkevich, and F. Le Normand, in: *Nanomagnetism*, J. M. Gonzalez Estevez (Ed.), Chap. 9, One Central Press, Manchester (2014), pp. 227–245.
4. A. L. Danilyuk, I. V. Komissarov, V. A. Labunov, F. Le Normand, A. Derory, J. M. Hernandez, J. Tejada, and S. L. Prischepa, *New J. Phys.*, **17**, 023073 (2015).
5. E. I. Kondorskii, *Dokl. Akad. Nauk SSSR*, **74**, 213–216 (1950).
6. S. N. Bokova, E. D. Obraztsova, V. V. Grebenyukov, K. V. Elumeeva, A. V. Ishchenko, and V. L. Kuznetsov, *Phys. Status Solidi B*, **247**, Nos. 11–12, 2827–2830 (2010).
7. I. V. Komissarov, I. A. Svito, A. K. Fedotov, and S. L. Prischepa, *Dokl. Nats. Akad. Nauk Belarusi*, **59**, No. 5, 31–37 (2015).
8. A. Atdayev, A. L. Danilyuk, and S. L. Prischepa, *Beilstein J. Nanotechnol.*, **6**, 1056–1064 (2015).